Are Polyelectrolyte Dendrimers Stimuli Responsive?

Giovanni Giupponi,[†] D. Martin A. Buzza,* and Dave B. Adolf[‡]

Department of Chemistry, University College London, London WC1H 0AJ, U.K., Department of Physics, University of Hull, Hull HU6 7FB, U.K., and School of Physics & Astronomy, University of Leeds, Leeds LS2 9JT, U.K.

Received March 13, 2007; Revised Manuscript Received June 6, 2007

ABSTRACT: Using a molecular dynamics and mean field theory approach which explicitly accounts for free ions, we study the conformation of polyelectrolyte dendrimers for different generation numbers, spacer lengths, charge distributions and ionic strengths. We find that, due to local charge neutrality, electrostatic interactions are strongly screened under all the conditions studied (including salt free conditions). This leads to the cores of the dendrimers being filled and to a very weak dependence of dendrimer conformations on ionic strength. These results are contrary the predictions of Debye−Hückel theory and highlight the limitations of Debye−Hückel theory in modeling the properties of highly charged macromolecular systems. However, our simulations suggest that some responsiveness to ionic strength may be recovered for more weakly charged dendrimers.

1. Introduction

Dendrimers are perfectly branched macromolecules where branching occurs hierarchically, each hierarchy adding to the generation number g of the dendrimer. Since their discovery in the 1980s, there has been a rapid growth of research in these novel materials due to their potential applications in a wide range of areas, including drug delivery, molecular catalysis, polymer therapeutics etc.[1−3] Recent interest in these novel macromolecules has focused on polyelectrolyte dendrimers. For example, when complexed with linear charged polymers such as DNA, polyelectrolyte dendrimers have been shown to act as "model histones"[4,5] and therefore have potential applications as nonviral vectors for gene delivery.[6] At the single molecule level, which is the focus of this paper, the seminal Monte Carlo simulation study of Welch and Muthukumar[7] suggests that polyelectrolyte dendrimers undergo a transition from a filled core conformation (i.e., terminal groups delocalized and the core is filled) to a "hollow core" conformation (i.e., terminal groups localized at the periphery and the core is hollow) with decreasing ionic strength. Similar results have also been obtained recently by Lyulin et al.[8] using Brownian dynamics simulations. These theoretical studies have attracted considerable interest for several reasons. First, they suggest that the hollow core conformation can be stabilized *energetically* using electrostatic interactions (for flexible neutral dendrimers, the ideal hollow core conformation[9] has been shown to be *entropically* unstable[10−14]). Second, they indicate that polyelectrolyte dendrimers can be used as stimuli responsive materials. Even so, the experimental status of these theoretical predictions remains unclear. For example, the small-angle neutron scattering (SANS) study by Nisato et al.[15] on $g = 8$ polyamidoamine (PAMAM) dendrimers (in the pH range where these molecules are charged) has found that the size of these macromolecules is essentially invariant with respect to ionic strength over the ionic strength range considered in refs 7 and 8.

* Author to whom correspondence should be addressed at the Department of Physics, University of Hull. E-mail: d.m.buzza@hull.ac.uk.

[†] Department of Chemistry, University College London. Current address: Computational Biochemistry and Biophysics Lab (GRIB−IMIM/UPF), Barcelona Biomedical Research Park (PRBB), C/ Dr. Aiguader 88, 08003, Barcelona, Spain. E-mail: giovanni.giupponi@upf.edu.

[‡] School of Physics & Astronomy, University of Leeds. E-mail: d.b.adolf@leeds.ac.uk.

In order to clarify this puzzling discrepancy between theory and experiment, in this paper, we performed a molecular dynamics (MD) study of polyelectrolyte dendrimers. The key difference between our study and the theoretical studies cited above[7,8] is the way in which Coulombic interactions are handled. In both refs 7 and 8 free ions are treated *implicitly* via the Debye−Hückel approximation. In this approximation, free ion degrees of freedom are integrated out, leaving the remaining charged monomer degrees of freedom to interact via a Yukawa potential with a screening length κ^{-1} (the Debye screening length) given by

$$\kappa^2 = 4\pi l_B \sum_i \rho_i z_i^2 \tag{1}$$

Here ρ_i and z_i are respectively the bulk number density and valence of the ith ion species and $l_B = e^2/(4\pi\epsilon k_B T)$ is the Bjerrum length of the dielectric medium with permittivity ϵ. The Debye−Hückel approximation has been very successful in describing interactions between charged colloids, both in the bulk[16] and in confined geometries.[17] It is also extensively used in the simulation of polyelectrolytes.[7,8,18] However although computationally very efficient, this approximation has several important limitations when dealing with polyelectrolytes. First, it implicitly assumes a constant free ion background (equal to the bulk free ion concentration), thus neglecting the tendency of free ions to repartition nonuniformly in order to minimize free energy.[19−21] Second, important nonlinear phenomena such as counterion condensation[22] are not captured by this theory. Both these limitations are likely to be relevant for the high bare charge densities encountered in typical polyelectrolyte dendrimers.

In order to circumvent these limitations, in this paper we use a simulation methodology that treats free ions *explicitly*.[20,21,23,24] The rest of the paper is organized as follows. In section 2, we provide details of our simulation model. In section 3, we present and discuss our simulation results and also construct a mean field model for charged dendrimers. Finally we summarize our conclusions in section 4.

2. Simulation Model

Using molecular dynamics simulations, we study the properties of charged dendrimers as a function of generation number

10.1021/ma070609l CCC: $37.00
Published on Web 07/12/2007

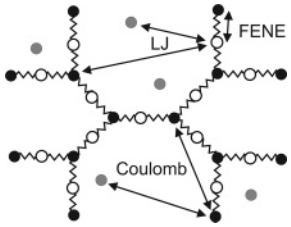

Figure 1. Explicit free ion model employed in this study for a $g = 3$, $s = 2$, case A dendrimer. Neutral monomers are white, charged monomers are black and free ions are gray. All particles interact with each other via a shifted Lennard-Jones (LJ) potential; connected nearest neighbor monomers interact via a finite nonlinear extensible elastic (FENE) potential; all charged particles interact with each other via a Coulomb potential.

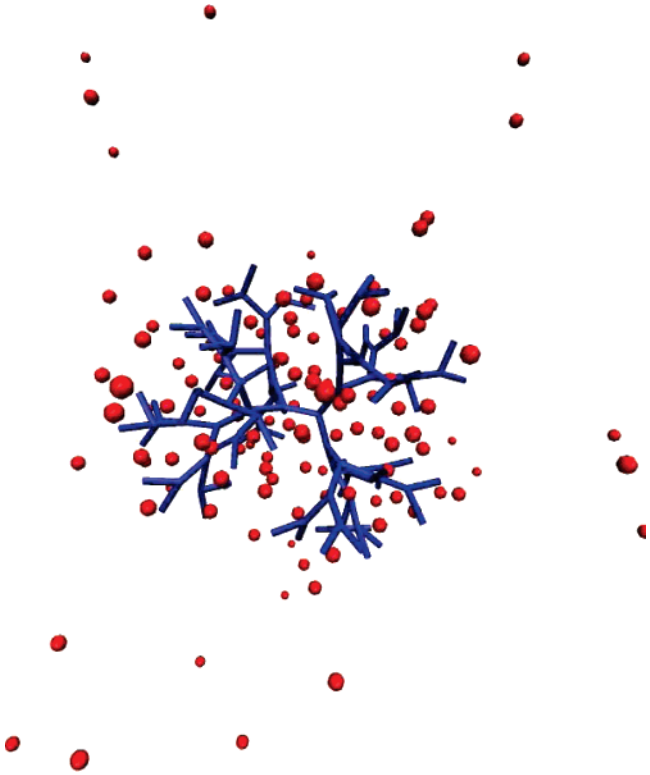

Figure 2. Snapshot of a $g = 5$, $s = 1$, case A dendrimer with no added salt.

g ($g = 3 \rightarrow 6$), the number of springs between branched monomers s ($s = 1, 2$) and ionic strength. We also consider three different charged monomer distributions, i.e., where all branched and terminal monomers are charged (case A), where only terminal monomers are charged (case B) and neutral. For PAMAM dendrimers, these cases correspond to low, intermediate and high pH values respectively.[25] The connectivity between monomers and interactions between particles (i.e., monomers, counterions, salt ions) used in our model are illustrated in Figure 1. A snapshot from our simulation is shown in Figure 2.

The charged dendrimers are modeled using a bead−spring model with implicit solvent and explicit counterions. We assume our dendrimers are in good solvent, and model the excluded volume interactions between all particles using a purely repulsive shifted Lennard-Jones (LJ) potential given by

$$V_{\mathrm{LJ}}(r) = \begin{cases} 4\epsilon_{\mathrm{LJ}}\left[\left(\frac{\sigma}{r}\right)^{12} - \left(\frac{\sigma}{r}\right)^{6} + \frac{1}{4}\right] & r \le 2^{1/6}\sigma \\ 0 & r > 2^{1/6}\sigma \end{cases} \quad (2)$$

where r denotes the separation between the particle centers. Note that the normal attractive part of the LJ potential is neglected by cutting off the potential at $r_{\mathrm{min}} = 2^{1/6}\sigma$ corresponding to the minima of the standard LJ potential. Note also that we have assumed the same LJ length for interactions between all particle pairs (i.e., monomer/monomer, monomer/free ion and free ion/free ion).[26] The simulation energy and length scales are respectively set by ϵ_{LJ} and σ and we work in units where $\epsilon_{\mathrm{LJ}} = \sigma = 1$.

To model bonded interactions, we assume that connected nearest neighbor monomers interact via the finite nonlinear extensible elastic (FENE) potential

$$V_{\mathrm{FENE}}(r) = \begin{cases} -\frac{1}{2}K\left(\frac{R_0}{\sigma}\right)^2 \ln\left[\left(1 - \left(\frac{r}{R_0}\right)^2\right)\right] & r \le R_0 \\ 0 & r > R_0 \end{cases} \quad (3)$$

where K denotes the spring constant and R_0 is the maximum bond length allowed. In order to prevent non-physical bond crossing, we set $R_0 = 1.5\sigma$ and $K = 30\epsilon_{\mathrm{LJ}}$.[27]

Finally all charged particles in the system interact via Coulomb interactions

$$V_{\mathrm{Coul}}(r) = l_{\mathrm{B}}k_{\mathrm{B}}T\frac{q_i q_j}{r_{ij}} \quad (4)$$

where q_i, q_j are the charges (in units of elementary charge e) carried by particles i and j which are separated by a distance r_{ij}. We assume that all charged particles in the system are monovalent so that $q_i = \pm 1$ (for definiteness, we assume that charged monomers carry positive charge). The Bjerrum length l_{B} is defined as the length at which the electrostatic energy equals the thermal energy and is given by $l_{\mathrm{B}} = e^2/(4\pi\epsilon k_{\mathrm{B}}T)$ where ϵ is the dielectric constant of the continuum medium. Since the Bjerrum length of water at room temperature is $l_{\mathrm{B}} = 7.1$ Å, we fix $l_{\mathrm{B}} = 1.25\sigma$. This yields $\sigma = 5.7$ Å, which is realistic for typical polyelectrolyte dendrimers in water.[7,8] The solvent molecules are treated as a continuum and taken into account only via the dielectric constant ϵ. Justification for treating the solvent molecules as a dielectric continuum comes from recent molecular dynamics (MD) studies of charged nanospheres in explicit water.[28] These simulations indicate that for spheres with charge and radii comparable to the LJ beads used in this study, the continuum description of electrostatic interactions (via a constant dielectric constant) is accurate for separations down to almost a single water molecule. Our assumption that ϵ is equal to that of *pure* solvent (water in this case) is justified *post hoc* by the fact that the calculated intramolecular monomer volume fractions ϕ are low ($\phi \approx 0.16$ for $s = 1$ and $\phi \approx 0.08$ for $s = 2$). The long-ranged Coulomb forces are calculated using the cell multipole P3M method.[29] This speeds up the standard Ewald summation technique from an order $O(N^{3/2})$ to an order $O(N \log N)$ calculation.

A single charged dendrimer was simulated in a cubic box with a typical box size of 30σ with periodic boundary conditions. For simulations on systems with no added salt, the box size was also varied up to 175σ in order to determine the effect of dendrimer and bulk free ion concentrations on single dendrimer conformations. The molecular dynamics (MD) simulations were performed using the ESPResSO package developed at the Max-Planck-Institute for polymer research in Mainz.[30] We perform NVT simulations using a Langevin thermostat setting the temperature to $k_{\mathrm{B}}T = 1.2\epsilon_{\mathrm{LJ}}$. The time step was set to $\Delta t = 0.002\tau$ (0.001τ for $g = 6$ simulations), where $\tau = \sqrt{m\sigma^2/\epsilon_{\mathrm{LJ}}}$ is

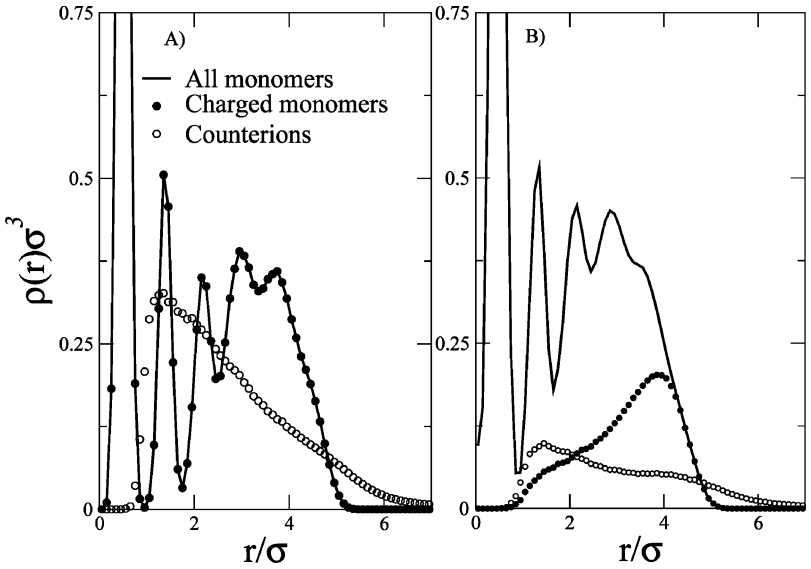

Figure 3. Normalized radial distribution profiles for different particle types for $g = 5$, $s = 1$ dendrimers with no added salt for case A (left) and B (right). Here r is the radial distance from the center of mass of the molecule.

the time unit in our simulation and $m = 1$ is the mass of the particles (we assume that all particles in the simulation have the same mass).

Initial configurations were generated using the following procedure. First, monomers were added one at a time at a distance σ from (but randomly oriented with respect to) connected monomers in the previous generation, starting from the $g = 0$ core and building up layer-wise to the required generation number. In the case of overlaps, another attempt is made to place the new monomer. We allow a maximum of 5000 attempts per particle. These random self-avoiding walk initial configurations were then annealed using a short MD run of around 1000 time-steps in order to separate any monomers that were placed too close to each other (a capped LJ potential was used during this run to avoid generating large forces that can break the FENE bonds). Salt ions, if present, are then inserted randomly. In the case of high salt concentration, salt ions are placed randomly but the system is evolved after each insertion with a very small integration time (typically 10 time-steps), setting all the particle velocities to zero in case the velocity of the fastest particle exceeds a threshold.

Having prepared our initial configuration, each simulation is run for 10^7 time-steps (2×10^6 in the case of high salt concentration). The first 30% of the simulation is used for equilibration. For the remainder of the run, dendrimer configurations were collected every 10^3 time-steps for analysis. We calculated the autocorrelation time for the radius of gyration R_g and found that the slowest relaxing (most correlated) $g = 6$ dendrimers decorrelate in less than 10^4 time-steps. This guarantees that we have (at least) about 10^3 independent samples for each simulation. The dendrimer configurations collected during the production run were then postprocessed to calculate radial distribution functions for different types of particles and the radius of gyration of the dendrimer.

3. Results and Discussion

3.1. Simulation Results. We first examine the conformation of charged dendrimers in the absence of added salt. In Figure 3, we plot the radial distribution function of all monomers (solid line), charged monomers (filled circles) and counterions (open circles) for a $g = 5$, $s = 1$ dendrimer for case A (left) and B (right). We define the radial distribution function as the average number density of a given type of particle at a radial distance r from the center of mass of the dendrimer. It is clear that the counterion profiles (open circles) are not uniform (as assumed by Debye−Hückel theory). This is also evident from the snapshot in Figure 2. The counterion profiles are also strikingly different between case A and case B even though the monomer profiles for the two cases are similar. This difference is largely correlated to differences in charged monomer profiles, the latter being very different for case A and B as one would expect. The correlation between counterion and charged monomer profiles is especially strong for case A though it is somewhat weaker for case B, presumably because of the lower charge density. It is nevertheless still present as can be seen from the fact that for case B, the small r peak in the counterion profile is strongly suppressed and the mean radial position of counterions is shifted to higher r.

The correlation between counterion and charged monomer profiles is a manifestation of the tendency of counterions to achieve local charge neutrality, a feature that is also seen in polyelectrolyte brushes and stars.[19−21] Local charge neutrality leads to internal counterion concentrations which are much higher than the bulk values, e.g., for our case A dendrimer, the internal counterion concentration is $\rho\sigma^3 \approx 0.2$, i.e., $\rho \approx 2$ M compared to a bulk counterion concentration of $\rho_0 = 0.04$ M (the latter arises from finite box size L of our simulation).

The tendency toward local charge neutrality in our systems can also be seen in Figure 4 where we plot the fraction of counterions lying within a distance $1.5R$ of the center of mass of a charged dendrimer as a function of g for different s and charge distributions under salt-free conditions ($R = \sqrt{5/3}R_g$ is the radius of a sphere with the same R_g as the dendrimer). We see that except at low g, the majority of counterions lie within $1.5R$ of the center of mass. We note that the fraction of counterions in or around a dendrimer are much higher than the values corresponding to a uniform distribution of counterions in the simulation box. For example for $g = 5$, $s = 1$, case A, the fraction of counterions lying within $1.5R$ is found from simulation (with simulation box size $L = 30\sigma$) to be 77% compared to 5% were the counterions uniformly distributed. The tendency toward local charge neutrality suggests that our dendrimers are in the so-called "osmotic brush" regime[18,19] where electrostatic interactions are strongly screened and the

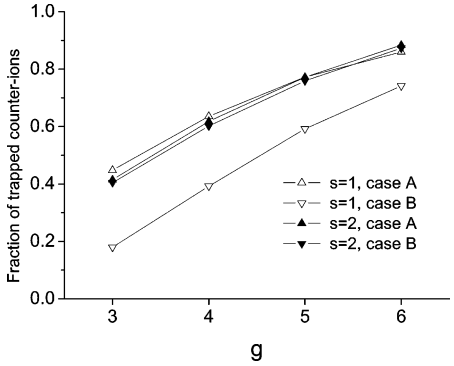

Figure 4. Fraction of "trapped" counterions, i.e., those lying within a distance $1.5R$ of the center of mass of a charged dendrimer as a function of g for different s and charge distributions under salt-free conditions ($R = \sqrt{5/3}R_g$ is the radius of a sphere with the same R_g as the dendrimer).

dominant energetic term is counterion osmotic pressure (we discuss this point in more detail in section 3.2).

Interestingly we do not observe a crossover from the osmotic regime to the "electrostatic regime" (i.e., where electrostatics is dominant) when we increase the simulation box size L to effectively infinity. For example for $g = 5$, $s = 1$, case A, even for $L = 175\sigma$, the majority of counterions (58%) still lie within $1.5R$ of the center of mass. This is consistent with the Poisson−Boltzmann calculations of Pincus[18,19] which show that provided the charge density is high enough, polyelectrolyte brushes remain in the osmotic regime (i.e., local charge neutrality valid) even at infinite dilution.

From Figure 3, it is also clear that the concentration profile for both case A and B dendrimers is filled core rather than hollow core. (The filled core profiles are modulated at small r by liquid-like ordering of monomers due to excluded volume interactions.) In contrast, Debye−Hückel theory predicts a hollow core configuration[7,8] since the Debye screening length associated with the bulk free ion concentration is comparable to dendrimer size in both cases (i.e., $\kappa^{-1} = 3.7\sigma$ vs $R_g = 3.6\sigma$ for case A and $\kappa^{-1} = 5.2\sigma$ vs $R_g = 3.4\sigma$ for case B). We also find that terminal groups are more strongly delocalized compared to the predictions of Debye−Hückel theory. For example from our simulations, the terminal group radius of gyration over the radius of gyration $R_{gt}/R_g = 1.13$ for case A and $R_{gt}/R_g = 1.12$ for case B. This compares with $R_{gt}/R_g > 2$ from Debye−Hückel theory for similar system parameters.[7] The filled core conformation that we observe is a consequence of local charge neutrality which, as we have explained earlier, leads to a stronger than expected screening of electrostatic interactions compared to Debye−Hückel theory. We note that the filled core conformation for polyelectrolyte dendrimers has also very recently been observed in a MD study by Terao[24] using explicit counterions.

Next, we examine the dependence of dendrimer conformation on ionic strength. In Figure 5 we plot the total (open symbols) and terminal (filled symbols) monomer concentration profiles for $g = 5$, case A dendrimers with a spacer length of $s = 1$ (left) and $s = 2$ (right) for bulk ionic strengths of $\rho_0 = 2 \times 10^{-4}$ M and $\rho_0 = 1$ M. These are respectively achieved using a simulation box size of $L = 175\sigma$ with no added salt (i.e., we use the background counterion concentration to mimic the effect of added salt) and $L = 30\sigma$ with the addition of 3000 salt ion pairs. Using eq 1, these ionic strengths correspond to nominal Debye screening lengths of $\kappa^{-1} = 300$ Å and $\kappa^{-1} = 3$ Å respectively. Debye−Hückel theory, therefore, predicts that the dendrimer should undergo a transition from filled core to hollow core conformation as we lower the ionic strength, and there should be a concomitant dramatic increase in dendrimer size.[7]

In fact for $s = 1$, both the total monomer and terminal monomer concentration show very weak variation with ionic strength. For example for $s = 1$, $g = 5$, R_g increases by about 4% going from high salt to low salt (specifically $R_g = 3.63\sigma$, 3.50σ for the low and high salt concentrations respectively). On the other hand for $s = 2$, some dependence on ionic strength is recovered, but the variation is much weaker than that predicted by Debye−Hückel theory. For example, for $s = 2$, $g = 5$, R_g increases by about 15% going from high salt to low salt (specifically $R_g = 5.99\sigma$, 5.22σ for the low and high salt concentrations respectively) compared to an increase of about 70% found using Debye−Hückel theory for similar system parameters.[7] The monomer concentration profiles are also filled core rather than hollow core at the lowest ionic strength. For example, for $s = 1$ and $s = 2$ we find $R_{gt}/R_g = 1.13$ compared to $R_{gt}/R_g > 2$ found using Debye−Hückel theory[7] for similar system parameters.

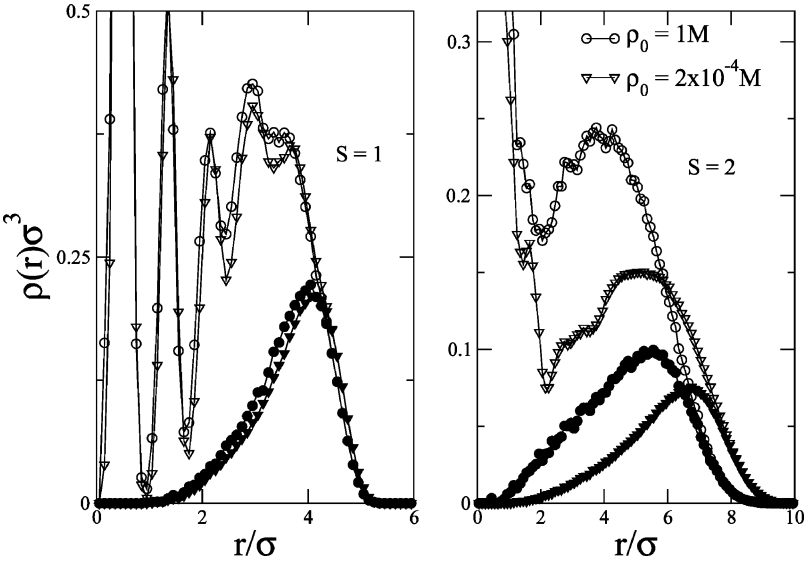

Figure 5. Normalized radial distribution profiles for all monomers (open symbols) and terminal monomers (filled symbols) for $g = 5$ case A dendrimers with $s = 1$ (left) and $s = 2$ (right) for different ionic strengths.

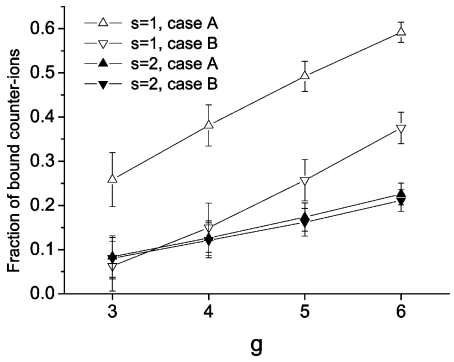

Figure 6. Fraction of bound counterions f_c as a function of g, s, and charge distribution in the absence of added salt. We define bound counterions as those lying within a distance l_B of a charged monomer.

The weak dependence of dendrimer conformations on ionic strength is again a consequence of our dendrimers being in the osmotic brush regime where the internal counterion concentration is high. Since the effective screening length is associated with the internal rather than bulk counterion concentration, the concentration of added salt needs to exceed the internal counterion concentration before we will see any appreciable change in dendrimer size. This fact was first pointed out by Pincus,[19] and it explains why polyelectrolyte brushes are so effective in stabilizing charged colloidal dispersions against salt induced aggregation (we will discuss this point in more detail in section 3.2). For the $s = 1$ case in Figure 5, we estimate that the internal concentration of delocalized counterions is $\rho \approx 1$ M (we define what we mean by delocalized at the end of this section). This is the same as the highest concentration of added salt we have used and explains why the $s = 1$ case only shows a very weak dependence on ionic strength. On the other hand, we estimate the internal concentration of delocalized counterions for the $s = 2$ case to be $\rho \approx 0.5$ M. This is lower than the highest concentration of added salt and explains why the $s = 2$ case exhibits a stronger degree of of variation with ionic strength.

Our simulations suggest that the ionic strength responsive behavior predicted by Debye−Hückel theory may be recovered by moving toward more weakly charged systems (e.g., by introducing long neutral spacers[31]). This is reasonable since Debye−Hückel theory becomes more accurate in this regime. However it is unclear whether electrostatic interactions are still strong enough in this regime to stabilize the hollow core conformation. We also note that the PAMAM dendrimers studied by Nisato et al.[15] correspond most closely with the $s = 1$ case in our model. We believe that this explains why essentially no variation in dendrimer size with ionic strength was found in these experiments.

One further limitation of Debye−Hückel theory is that it is a linearized theory which assumes that Coulombic interactions are everywhere weak. However as discussed in the introduction, this assumption is questionable for the high charge densities encountered in typical polyelectrolyte dendrimers. To illustrate this, in Figure 6 we plot the average fraction of counterions lying within a distance l_B of a charged monomer (f_c) as a function of g for different s and charge distributions under salt-free conditions. From eq 4, the electrostatic attraction between these counterions and the relevant charged monomers is greater than k_BT so that the counterions are effectively bound to the charged monomer. This is analogous to counterion condensation (or Manning condensation) observed in charged rods.[22] However in contrast to counterion condensation, the binding in our system is rather loose since the electrostatic attraction at contact ($r = \sigma$) is only $1.25k_BT$. We therefore refer to the fraction f_c of counterions as "bound" , reserving the term "counterion condensation" for situations where the binding is much stronger (i.e., many k_BT). We see that for all the parameters considered in our study, a significant fraction of counterions are bound, especially for case A and high g. This important feature of charged dendrimers is again not captured by Debye−Hückel theory.

3.2. Mean Field Theory. In the preceding section, we argued that the key driving forces controlling the conformation of charged dendrimers are local charge neutrality and the resultant (high) osmotic pressure of the trapped counterions. In order to check that these arguments are quantitatively reasonable, in this section we construct a minimal mean field model for charged dendrimers which explicitly accounts for free ions, both in the absence and in the presence of added salt.

As our baseline, we first consider the free energy of the dendrimer in the absence of charge. For this we use the Boris−Rubinstein model for neutral dendrimers[11] where the free energy of the dendrimer is

$$\beta F_0 = \frac{3N}{2(g + {}^1/_2)s}\frac{R^2}{R_0{}^2} - \frac{3N}{(g + 1/2)s}\ln\left(\frac{R}{R_0}\right) + \frac{3\upsilon N^2}{8\pi R^3} \quad (5)$$

Here $\beta = 1/k_BT$, $N = 4s(2^g - 1) + s + 1$ is the total number of monomers, R is the end-to-end distance of a linear strand emanating from the core of the dendrimer (i.e., the midpoint of the central cross-bar), $R_0{}^2 = (g + 1/2)s\sigma^2$ is the Gaussian size of the linear strand and υ is the excluded volume parameter. The first and second terms in eq 5 give the entropic contribution to the free energy due to stretching and compressing the dendrimer respectively while the third term is the excluded volume interaction energy between monomers (we assume good solvent conditions so that three and higher body terms can be neglected).

In the absence of salt, the free energy of the charged dendrimer is obtained by adding the counterion contribution to the baseline model and imposing charge neutrality. This yields

$$\beta F = \beta F_0 + N_c\left[\ln\left(\frac{3N_c}{4\pi R^3}\sigma^3\right) - 1\right] \quad (6)$$

where N_c is the effective number of delocalized (i.e., unbound) counterions within the dendrimer. The specific value that we use for N_c will be discussed in more detail later. The second term on the rhs of eq 6 is the translational entropy of delocalized counterions within the dendrimer (for simplicity, we have neglected any nonideality of the counterions). Note that we have neglected the effect of electrostatics in our model because we argue that these are strongly screened due to local charge neutrality. Instead, as first pointed out by Pincus,[19] the dominant role of electrostatics in polyelectrolyte brush systems is to preserve local charge neutrality. This incurs an entropic penalty because the neutralizing counterions are effectively trapped within the dendrimer and are prevented from exploring the volume outside the dendrimer. This effect gives rise to counterion osmotic pressure which swells the dendrimer. The dominance of counterion osmotic pressure over explicit electrostatics in polyelectrolyte brushes (i.e., the "osmotic regime") has been confirmed by the Poisson−Boltzmann calculations of Pincus[19] and the microscopic simulations and analytical calculations of Jusufi et al.[20,21] on charged stars.

Note that in eq 6, we have also neglected the translational entropy of bound counterions (due to their mobility along the

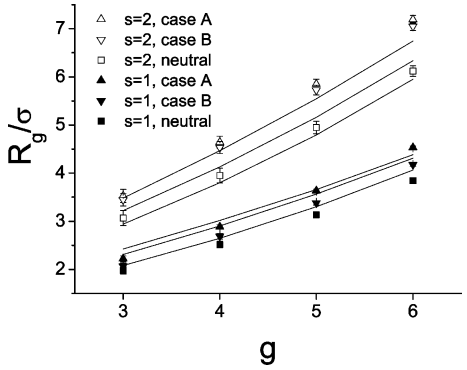

Figure 7. Simulation results for R_g vs g for $s = 1$ (filled symbols) and $s = 2$ (open symbols) for case A, case B and neutral dendrimers with no added salt. The solid lines are the predictions of the Flory theory (eq 7) using $\upsilon = 1.3\sigma^3$ and $\beta = 0.4$. See text for further details.

dendrimer backbone) because while this is important in determining the fraction of bound counterions f_c (see later), it does not couple directly to dendrimer size R. Minimizing the free energy in eq 6 with respect to R, the equilibrium size of the dendrimer is given in terms of the linear expansion factor ($\alpha = R/R_0 = R_g/R_{g0}$) via the equation

$$\alpha^5 - \alpha^3 - \frac{3\upsilon N}{8\pi[(g+1/2)s]^{1/2}} = \frac{(g+1/2)s}{N} N_c \alpha^3 \qquad (7)$$

where R_{g0} is the Gaussian radius of gyration of the dendrimer which can be readily calculated using the recursive method of Wallace et al.[32] (see appendix).

Finally, we turn to the choice of the effective number of delocalized counterions N_c in eq 7. In a more sophisticated theory, N_c would be determined self-consistently by including terms such as the translational entropy and electrostatic interaction energy of bound counterions in the free-energy minimization.[20,21] In this paper, we take a simpler approach where we fix N_c from simulation. Specifically we set $N_c = \gamma N_{c0}(1 - f_c)$ where f_c is the fraction of bound counterions determined from simulation (i.e., Figure 6), N_{c0} is the total number of counterions ($N_{c0} = 2(2^{g+1} - 1)$ for case A, $N_{c0} = 2^{g+1}$ for case B and $N_{c0} = 0$ for neutral dendrimers), and γ is a scaling factor which we use as a fitting parameter.

In Figure 7, we plot our simulation results (symbols) for R_g vs g for $s = 1$, 2, case A, case B and neutral dendrimers with no added salt. The data was then fitted to eq 7 using υ and γ as fitting parameters and the best fits (solid lines) were found for $\upsilon = 1.3\sigma^3$ and $\gamma = 0.4$. Given the minimal nature of the theory, the fits to the simulation data are reasonably good. In particular for both $s = 1$, 2, the theory captures the correct trend for R_g vs g and the correct order of magnitude for dendrimer swelling.

Next we consider the free energy of the charged dendrimer in the presence of salt. This is obtained by adding in the contribution of the salt counter- and co-ions to eq 6. Imposing charge neutrality as before, the total free energy of the dendrimer is now given by

$$\beta F = \beta F_0 + (N_c + N_s)\left[\ln\left(\frac{3(N_c+N_s)}{4\pi R^3}\sigma^3\right) - 1\right] + N_s\left[\ln\left(\frac{3N_s}{4\pi R^3}\sigma^3\right) - 1\right] \qquad (8)$$

where N_s is the number of salt ion pairs within the dendrimer (as in our simulations, we assume the salt to be monovalent). Note that the salt concentration *within* the dendrimer $3N_s/(4\pi R^3)$ will in general be different from the value in the bulk ρ_0 due to salt repartitioning between the dendrimer and the bulk (i.e., the Donnan effect[33,34]). To determine N_s and R, we equate the osmotic pressure of the dendrimer to that of the salt ions in the bulk (i.e., mechanical equilibrium) and equate the salt chemical potential in the dendrimer to that in the bulk (i.e., chemical equilibrium for salt ions).

The chemical potential of salt ion pairs in the dendrimer is found by differentiating F given by eq 8 with respect to N_s at fixed R (i.e., dendrimer volume)

$$\beta\mu_s = \beta\frac{\partial F}{\partial N_s} = \ln\left(\frac{3(N_c+N_s)}{4\pi R^3}\sigma^3\right) + \ln\left(\frac{3N_s}{4\pi R^3}\sigma^3\right) \qquad (9)$$

Equating μ_s to the bulk salt chemical potential $\mu_{s0} = 2k_BT \ln(\rho_0\sigma^3)$ we find

$$\rho_0^{\,2} = \frac{3N_s}{4\pi R^3}\cdot\frac{3(N_c+N_s)}{4\pi R^3} \qquad (10)$$

This is the usual Donnan equilibrium equation which allows us to determine N_s. Solving for N_s we find

$$N_s = \frac{1}{2}\left[(N_c^{\,2} + N_0^{\,2}\alpha^3)^{1/2} - N_c\right] \qquad (11)$$

where $N_0 = 2\rho_0 4\pi R_0^3/3$ and $\alpha = R/R_0$ as before.

The osmotic pressure of the dendrimer is found by differentiating F with respect to dendrimer volume $V = 4\pi R^3/3$ at fixed N_s, i.e.,

$$\Pi = -\frac{\partial F}{\partial V} = -\frac{1}{4\pi R^2}\frac{\partial F}{\partial R} \qquad (12)$$

Equating the resultant expression for Π to the bulk salt osmotic pressure $2\rho_0 k_BT$ and substituting eq 11 for N_s, we find after some algebra that the equilibrium size of polyelectrolyte dendrimers in the presence of salt is given by

$$\alpha^5 - \alpha^3 - \frac{3\upsilon N}{8\pi[(g+1/2)s]^{1/2}} = \frac{(g+1/2)s}{N} \times \alpha^3[(N_c^{\,2} + N_0^{\,2}\alpha^6)^{1/2} - N_0\alpha^3] \qquad (13)$$

In the low salt regime ($N_0 \ll N_c$), we recover the salt free result given by eq 7. On the other hand in the high salt regime ($N_0 \gg N_c$), we recover the result for neutral dendrimers (i.e., *rhs* of eq 13 equal to zero).[11] Eq 13 is thus physically reasonable across the entire range of salt concentrations.

Note that for typical polyelectrolyte dendrimers and salt concentrations, N_c is much larger than N_0 so that we are in the low salt regime where dendrimer size is only weakly dependent on ionic strength. To illustrate this we use eq 13 and values of N_c derived from our salt free simulations to calculate the change of dendrimer size with ionic strength for $g = 5$, case A dendrimers (i.e., Figure 5). For $s = 1$ ($N_c \approx 25$) our mean field theory predicts $R = 3.66\sigma$ for $\rho_0 = 2 \times 10^{-4}$ M ($N_0 = 0.002$) and $R = 3.37\sigma$ for $\rho_0 = 1$ M ($N_0 \approx 12$), i.e., an increase of 9% going from high to low salt. On the other hand, for $s = 2$ ($N_c \approx 41$), our mean field theory predicts $R = 5.55\sigma$ for $\rho_0 = 2 \times 10^{-4}$ M ($N_0 = 0.007$) and $R = 4.86\sigma$ for $\rho_0 = 1$ M ($N_0 \approx 34$), i.e., an increase of 14% going from high to low salt. The predicted increases are in good agreement with the values found from simulation (4% and 15% for $s = 1$, 2 respectively) but significantly smaller than the increase predicted by Debye−Hückel theory (typically 70%).[7]

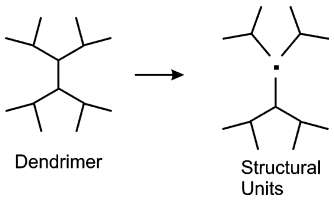

Figure 8. Structural units used to calculate the scattering form factor for a $g = 2$ dendrimer.

In summary, we obtain quantitative agreement between the explicit free ion mean field theory and our simulation data. The mean field model therefore supports our argument that for our dendrimer parameters (which are typical for polyelectrolyte dendrimers), we are in the osmotic brush regime where Coulombic interactions are strongly screened and the dominant driving force for swelling comes from the osmotic pressure of delocalized counterions.

4. Conclusions

Using a molecular dynamics approach which explicitly accounts for counterions, we find that the conformation of typical polyelectrolyte dendrimers is dense core (rather than hollow core) and only very weakly dependent on ionic strength. These results are contrary to implicit free ion simulations based on Debye−Hückel theory[7,8] but are in agreement with current experiments.[15] Analysis of our simulation results and an explicit free ion mean field model indicates that these results are due to the tendency in charged dendrimers toward local charge neutrality which leads to stronger than expected screening of electrostatic interactions and high internal counterion concentrations, even in the absence of added salt. This important piece of physics is missed in Debye−Hückel theory. The limitation of Debye−Hückel theory for modeling dense polyelectrolyte systems such as planar brushes and stars is already known. Evidently typical polyelectrolyte dendrimers should be added to this list of charged systems where one needs to explicitly account for free ion degrees of freedom in the modeling. Finally, our simulations suggest that if the bare charge density of polyelectrolyte dendrimers is decreased (e.g., by introducing long neutral spacers), some responsiveness to ionic strength may be recovered. We hope our study will stimulate future experimental studies in this direction.

Appendix A. Calculation of Gaussian Radius of Gyration

In this appendix we briefly outline how the Gaussian radius of gyration of our dendrimers R_{g0} can be calculated using the recursive method of Wallace et al.;[32] full details of the method can be found in ref[32]. The connectivity of our dendrimer and relevant "structural units" used in the calculation are shown in Figure 8; note that these are slightly different from those used in ref 32. Denoting J_g and H_g as the "self-term" and "co-term" respectively of a generation g dendritic branch, the scattering form factor for a generation g dendrimer is given by

$$P_g(q) = J_g + 2J_{g-1} + 1 + 4H_gH_{g-1} + 2H_{g-1}H_{g-1} + 4H_{g-1} + 2H_g \quad (14)$$

The first three terms account for self-correlations within the generation g dendritic branch (first term), the two generation $g - 1$ dendritic branches (second term) and the core monomer (third term). The fourth and fifth terms account for correlations between the different dendritic branches. The sixth and seventh terms account for correlations between the core monomer and the different dendritic branches.

Expressions for H_g, J_g (as well as J_0, H_0, G_0, which are respectively the self-term, co-term and propagator for a spacer) are given in ref[32] so that it is straightforward to calculate $P_g(q)$ using eq 14. Finally, the Gaussian radius of gyration R_{g0} for a generation g dendrimer is obtained by Taylor expanding $P_g(q)$ to second order in q

$$P_g(q) = 1 - \frac{1}{3}q^2R_{g0}{}^2 + O(q^4) \quad (15)$$

The resultant analytic expressions for R_{g0} are straightforward but long and are therefore not reproduced here.

References and Notes

(1) Frechet, J. M. J. *Science* **1994**, *263*, 1710.
(2) Bosman, A. W.; Janssen, H. M.; Meijer, E. W. *Chem. Rev.* **1999**, *99*, 1665.
(3) Duncan, R. *Nat. Rev. Drug Discovery* **2003**, *2*, 347.
(4) Welch, P.; Muthukumar, M. *Macromolecules* **2000**, *33*, 6159.
(5) Evans, H. M.; Ahmad, A.; Ewert, K.; Pfohl, T.; Martin-Herranz, A.; Bruinsma, R. F.; Safinya, C. R. *Phys. Rev. Lett.* **2003**, *91*, 075501.
(6) Kukowska-Latallo, J. F.; Bielenska, A. U.; Jonson, J.; Spindler, R.; Tomalia, D. A.; Baker, J. R., Jr. *Proc. Natl. Acad. Sci. U.S.A.* **1996**, *93*, 4897.
(7) Welch, P.; Muthukumar, M. *Macromolecules* **1998**, *31*, 5892.
(8) Lyulin, S. V.; Evers, L. J.; van der Schoot, P.; Darinskii, A. A.; Lyulin, A. V.; Michels, M. A. J. *Macromolecules* **2004**, *37*, 3049.
(9) de Gennes, P. G.; Hervet, H. J. *J. Phys. Lett.* **1983**, *44*, L351.
(10) Lescanec, R. L.; Muthukumar, M. *Macromolecules* **1990**, *23*, 2280.
(11) Boris, D.; Rubinstein, M. *Macromolecules* **1996**, *29*, 7251.
(12) Zook, T. C.; Pickett, G. T. *Phys. Rev. Lett.* **2003**, *90*, 015502.
(13) Potschke, D.; Ballauff, M.; Lindner, P.; Fischer, M.; Vogtle, F. *Macromol. Chem. Phys.* **2000**, *201*, 330.
(14) Rosenfeldt, S.; Dingenouts, N.; Ballauff, M.; Werner, N.; Vogtle, F.; Lindner, P. *Macromolecules* **2002**, *35*, 8098.
(15) Nisato, G.; Ivkov, R.; Amis, E. J. *Macromolecules* **2000**, *33*, 4172.
(16) Israelachvili, J. *Intermolecular & Surface Forces*, 2nd ed.; Academic Press: London, 1991.
(17) Baumgartl, J.; Arauz-Lara, J. L.; Bechinger, C. *Soft Matter* **2006**, *2*, 631.
(18) Netz, R. R.; Andelman, D. *Phys. Rep.* **2003**, *380*, 1.
(19) Pincus, P. *Macromolecules* **1991**, *24*, 2912.
(20) Jusufi, A.; Likos, C. N.; Lowen, H. *Phys. Rev. Lett.* **2002**, *88*, 018301.
(21) Jusufi, A.; Likos, C. N.; Lowen, H. *J. Chem. Phys.* **2002**, *116*, 11011.
(22) Manning, G. S. *J. Chem. Phys.* **1969**, *51*, 954.
(23) Gurtovenko, A. A.; Lyulin, S. V.; Karttunen, M.; Vattulainen, I. *J. Chem. Phys.* **2006**, *124*, 094904.
(24) Terao, T. *Mol. Phys.* **2006**, *104*, 2507−2513.
(25) Cakara, D.; Kleimann, J.; Borkovec, M. *Macromolecules* **2003**, *36*, 4201.
(26) We have also studied the more realistic but complicated case where the LJ length for free ion/free ion (σ_{ii}) and free ion/monomer (σ_{im}) interactions are smaller than that for monomer/monomer interactions (σ_{mm}), specifically $\sigma_{ii} = \sigma_{im} = \sigma_{mm}/2.4$. This yields qualitatively the same results as the case $\sigma_{ii} = \sigma_{im} = \sigma_{mm} = \sigma$. For simplicity, we therefore only present results for equal LJ length in this paper.
(27) Harreis, H. M.; Likos, C. N.; Ballauff, M. *J. Chem. Phys.* **2003**, *118*, 1979.
(28) Dzubiella, J.; Hansen, J.-P. *J. Chem. Phys.* **2003**, *119*, 12049.
(29) Hockney, R. W.; Eastwood, J. W. *Computer simulation using particles;* IOP: 1988.
(30) Limbach, H. J.; Arnold, A.; Mann, B. A.; Holm, C. *Comput. Phys. Commun.* **2006**, *174*, 704.
(31) Hutchings, L.; Roberts-Bleming, S.; Dodds, J. *Macromolecules* **2005**, *38*, 5970.
(32) Wallace, E. J.; Buzza, D. M. A.; Read, D. J. *Macromolecules* **2001**, *34*, 7140.
(33) Donnan, F. G. *Elektrochem.* **1911**, *17*, 572.
(34) Warren, P. B. *J. Phys.: Condens. Matter* **2002**, *14*, 7617−7629.

MA070609L